The American Journal of Pathology, Vol. 169, No. 4, October 2006

DOI: 10.2353/ajpath.2006.051250

Neurobiology

Cortical Neuronal and Glial Pathology in TgTau^{P301L} Transgenic Mice

Neuronal Degeneration, Memory Disturbance, and Phenotypic Variation

Tetsuro Murakami,* Erwan Paitel,† Takeshi Kawarabayashi,* Masaki Ikeda,‡ M. Azhar Chishti,† Christopher Janus,† Etsuro Matsubara,§ Atsushi Sasaki,¶ Toshitaka Kawarai,† Amie L. Phinney,† Yasuo Harigaya,‖ Patrick Horne,† Nobuaki Egashira,** Kenichi Mishima,** Amanda Hanna,† Jing Yang,† Katsunori Iwasaki,** Mitsuo Takahashi,†† Michihiro Fujiwara,** Koichi Ishiguro,‡‡ Catherine Bergeron,† George A. Carlson,§§ Koji Abe,* David Westaway,† Peter St. George-Hyslop,† and Mikio Shoji*

From the Department of Neurology, Neuroscience and Biophysiological Science, Okayama University Graduate School of Medicine, Dentistry, and Pharmaceutical Sciences, Okayama, Japan; the Department of Neurology‡ and First Department of Pathology,¶ Gunma University Graduate School of Medicine, Gunma, Japan; the Department of Alzheimer's Disease Research,§ National Institute of Longevity Sciences, National Center for Geriatrics and Gerontology, Aichi, Japan; the Department of Neurology,‖ Maebashi Red Cross Hospital, Gunma, Japan; the Departments of Clinical Pharmacology‡† and Neuropharmacology,** Faculty of Pharmaceutical Sciences, Fukuoka University, Fukuoka, Japan; the Alzheimer's Disease Group,‡‡ Mitsubishi Kagaku Institute of Life Sciences, Tokyo, Japan; the Departments of Medicine (Neurology) and Laboratory Medicine and Pathobiology,† Centre for Research in Neurodegenerative Diseases, University of Toronto, Toronto, Ontario, Canada; and the McLaughlin Research Institute,§§ Great Falls, Montana*

Recapitulation of tau pathologies in an animal model has been a long-standing goal in neurodegenerative disease research. We generated transgenic (TgTau^{P301L}) mice expressing a frontotemporal dementia with parkinsonism linked to chromosome 17 (FTPD-17) mutation within the longest form of tau (2N, 4R). TgTau^{P301L} mice developed florid pathology including neuronal pretangles, numerous Gallyas-Braak-positive neurofibrillary tangles, and glial fibrillary tangles in the frontotemporal areas of the cerebrum, in the brainstem, and to a lesser extent in the spinal cord. These features were accompanied by gliosis, neuronal loss, and cerebral atrophy. Accumulated tau was hyperphosphorylated, conformationally changed, ubiquitinated, and sarkosyl-insoluble, with electron microscopy demonstrating wavy filaments. Aged TgTau^{P301L} mice exhibited impairment in hippocampally dependent and independent behavioral paradigms, with impairments closely related to the presence of tau pathologies and levels of insoluble tau protein. We conclude that TgTau^{P301L} mice recreate the substantial phenotypic variation and spectrum of pathologies seen in FTDP-17 patients. Identification of genetic and/or environmental factors modifying the tau phenotype in these mice may shed light on factors modulating human tauopathies. These transgenic mice may aid therapeutic development for FTDP-17 and other diseases featuring accumulations of four-repeat tau, such as Alzheimer's disease, corticobasal degeneration, and progressive supranuclear palsy. ***(Am J Pathol 2006, 169:1365–1375; DOI: 10.2353/ajpath.2006.051250)***

Supported by the Ministry of Health, Labor, and Welfare of Japan (grants-in-aid for Primary Amyloidosis Research Committee to S.I. and grants to Y.I, T.I., and S.K.); the Ministry of Education, Culture, Sports, Science, and Technology, Japan (grants-in-aid for scientific research: B, 16390251 and 1590273; C, 16590829; Hoga, 17659445; the National Project on Protein Structural and Function Analyses and Scientific Research on Priority Areas, C, Advanced Brain Science Project); the Canadian Institutes for Health Research; the Canadian Foundation for Innovation; the Alzheimer's Societies of Ontario and Saskatchewan; and by the Alzheimer's Association.

Accepted for publication June 22, 2006.

Supplementary material for this article can be found on *http://ajp.amjpathol.org*.

Address reprint requests to Mikio Shoji, M.D., Ph.D., Department of Neurology, Neuroscience, Biophysiological Science, Okayama University Graduate School of Medicine and Dentistry, 2-5-1 Shikata-cho, Okayama, 700-8558 Japan, or Prof. David Westaway, Westaway Lab, Alberta Centre for Prions and Protein Folding Disorders, Room 222A, Environmental Engineering Building, University of Alberta, Edmonton, AB T6G 2G2 Canada. E-mail: mshoji@cc.okayama-u.ac.jp and david.westaway@utoronto.ca.

Frontotemporal dementia with parkinsonism linked to chromosome 17 (FTDP-17) is characterized by the insidious onset of behavioral and personality changes with dementia and parkinsonism.[1] Some cases have been reported as Alzheimer's disease (AD)-like dementias accompanied by various degrees of parkinsonism and psychiatric symptoms[2–4], whereas others have been described as Pick's disease,[5,6] corticobasal degeneration (CBD),[7] or progressive supranuclear palsy (PSP).[8] FTDP-17 patients show atrophy, with severe neuronal loss, astrocytosis, and spongiosis in the frontotemporal lobe, and various degrees of degeneration in the subcortical nuclei. Tau-associated pathology is prominent in the form of numerous tau-positive pretangles, some neurofibrillary tangles (NFTs), and extensive glial fibrillary tangles (GFTs). In addition, tau protein shifts from the sarkosyl-soluble fraction into sarkosyl-insoluble deposits.[9] Although FTDP-17 is caused by mutations in the single gene tau, the clinical and pathological features are markedly different among patients carrying distinct mutations and often even among patients within the same family.[7,10,11]

Several lines of transgenic mice (Tg) that show NFT-like structures or tau-positive inclusions in the brain and spinal cord have been generated, although few of them show the major pathological features of FTDP-17.[12–15] Tau P301L is the mutation observed most frequently in FTDP-17.[3,11,16–18] We report here a line of transgenic mice expressing a P301L mutant version of the longest form of human tau [denoted TgTau(P301L)23027, for brevity TgTau^{P301L}] that developed pretangles and numerous GFTs and NFTs with pathological features seen in FTDP-17. The age-related appearance of NFTs and GFTs was closely related to neuronal and synaptic losses with cerebral atrophy and impaired hippocampal-dependent explicit spatial and working memory, as well as hippocampal-independent implicit associative learning.

Materials and Methods

Generation of Tg Mice Expressing P301L Human Tau

The longest isoform of human 2N4R wild-type (wt) tau cDNA containing a eukaryotic Kozak initiation sequence[19] upstream of the start codon was ligated to the *Sal*I-digested site of a linearized cos.Tet expression vector containing the Syrian hamster prion protein gene promoter,[20,21] packaged *in vitro*, and plated on *Escherichia coli* DH1 to obtain a bacterial stock containing the recombinant cosmid clone (Figure 1). Similar procedures were adopted for a P301L mutant construct. Transgene inserts were purified, digested, and microinjected into fertilized oocytes of 129SvEv × FVB/N F1 mice, as previously described,[21] and then the resultant mice were backcrossed to 129 mice. A short noncoding region (~100 bp) was also included in the transgene.[22] In the case of the P301L construct, one Tg line was obtained, and first generation offspring were used to start two breeding colonies. All animal experiments were performed according to guidelines established in the Guide for the Care and Use of Laboratory Animals (Japan) and Canadian Council on Animal Care guidelines (Canada).

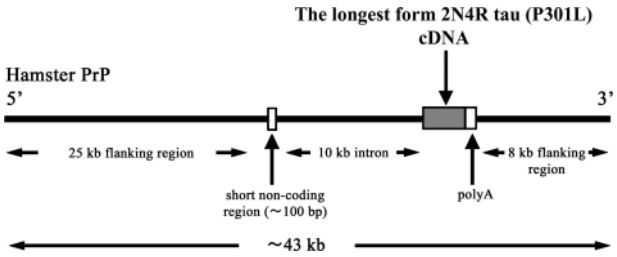

Figure 1. Structure of the cos.Tet-derived Tau 2N4R transgene used to construct TgTau^{P301L} mice. Exonic sequences are denoted by boxes. Figure is not to scale.

Histological Study

After mice were sacrificed under anesthesia, the brains were removed and cut sagittally on the midline. One hemisphere was fixed in 0.1 mol/L phosphate buffer (pH 7.6) containing 4% paraformaldehyde and embedded in paraffin. For immunostaining, sections were treated with 99% formic acid for 3 minutes. After blocking with 5% normal goat or horse serum in 50 mmol/L phosphate-buffered saline (PBS) containing 0.05% Tween-20 and 4% Block-Ace (Snow Brand, Sapporo, Japan), sections were incubated with primary antibodies for 6 hours. The specific labeling was visualized using a Vectastain Elite ABC kit (Vector Laboratories, Burlingame, CA). Immunostained tissue sections were counterstained with hematoxylin.

Five-μm coronal hemisphere sections were used for hematoxylin and eosin (H&E), Gallyas-Braak, Bielschowsky, Bodian, thioflavin-S, and Nissl staining. The following antibodies were used for immunostaining: Tau154 (a polyclonal antibody against amino acids 154 to 168 of human tau 441, 1:200), tau-C (a polyclonal antibody against C-terminal amino acids 422 to 438 of both human and mouse tau, 1:200), and Alz50 (an antibody against paired-helical-filament tau, 1:100).[23] CP27 (all forms of human tau, 1:500), MC1 (early epitope of conformationally changed tau, 1:500), and Tg3 (an Alzheimer-specific conformation of pThr231 tau, 1:50) were also used.[24] For the detection of phosphorylated tau, PS199 (serine-199, 1:500), AT8 (serine-202/threonine-205, 1:200; Innogenetics, Ghent, Belgium), and PHF1 (serine-396/serine-404, 1:100) were used.[23,24] Antibodies against glial fibrillary acidic protein (GFAP) (1:2000; DAKO, Glostrup, Denmark), synaptophysin (1:400, DAKO) and ubiquitin (Ubi-Q, 1:500)[25] were also used. Immunofluorescence study was performed with antibodies for tau and glial markers. The samples were incubated with AT8 and either anti-GFAP antibody or Olig2 (a marker for oligodendrocytes, 1:500; IBL, Fujioka, Japan) overnight at room temperature. Then the samples were incubated with fluorescein isothiocyanate-labeled (1:2000; Vector Laboratories) and rhodamine-labeled (1:2000; Chemicon, Temecula, CA) secondary antibody for 3 hours. The sections were examined by immunofluorescence microscopy (BX-51; Olympus, Tokyo, Japan).

For electron microscopy, tissue blocks from the brains of 14-month-old TgTau^{P301L} mice were immersed in 2.5% glutaraldehyde, 0.1 mol/L phosphate buffer, pH 7.4, for 4 hours and washed in 0.1 mol/L phosphate buffer containing 7% sucrose. The blocks were then postfixed in 2% osmium tetroxide, dehydrated in ethanol and propylene oxide, and embedded in Quetol 812 (Nisshin EM, Tokyo, Japan). Ultrathin sections were stained with uranyl acetate and lead acetate before observation. For immunoelectron microscopy, pre-embedding was performed. In brief, samples were fixed in periodate-lysine-paraformaldehyde at 4°C, washed in PBS containing graded concentrations of sucrose, and rapidly frozen in liquid nitrogen. The sections (6 to 8 μm) were incubated with AT8 antibody followed by anti-mouse IgG F(ab′)$_2$ conjugated with peroxidase (Vector Laboratories). After immunostaining, the sections were embedded in Quetol 812, and ultrathin sections were prepared. They were observed without additional staining by electron microscopy.

Western Blotting

Half of each brain was homogenized in 9 vol of Tris-saline buffer with the protease inhibitors [50 mmol/L Tris-HCl and 150 mmol/L NaCl, pH 7.6, 0.5 mmol/L diisopropyl fluorophosphate (DIFP), 0.5 mmol/L phenylmethyl sulfonyl fluoride, 1 μg/ml *N*-tosyl-L-lysine chloromethyl ketone (TLCK), 1 μg/ml antipain, 1 μg/ml leupeptin, 0.1 μg/ml pepstatin, and 1 mmol/L ethylene glycol bis(β-aminoethyl ether)-*N*,*N*,*N*′,*N*′-tetraacetic acid (EGTA)] and centrifuged at 55,000 rpm for 60 minutes at 4°C. The supernatant was analyzed as the Tris saline buffer-soluble fraction. The pellet was homogenized again in 4 vol of 1% sarkosyl in Tris saline inhibitors, incubated on ice for 30 minutes, and centrifuged at 55,000 rpm for 60 minutes at 4°C. The pellet was analyzed as the sarkosyl-insoluble fraction. The samples were boiled at 70°C in 4 vol of sodium dodecyl sulfate sample buffer and separated on 4 to 12% NuPAGE Bis-Tris gel (Invitrogen, Carlsbad, CA), and the blots were probed with antibodies tau-C, Tau154, CP27, Alz50, MC1, AT8, or Tg3. Signals were visualized with an enhanced chemiluminescence detection system (Amersham, Buckinghamshire, UK) and quantified using a luminoimage analyzer (LAS 1000-mini; Fuji Film, Tokyo, Japan).

Behavioral Experiments

TgTau^{P301L} and non-Tg littermates in Okayama (TgTau$^{P301L(O)}$) were enrolled in behavioral experiments. In this cohort, the Morris water-maze (MWM) test was performed at ages 9 and 12 months for reference and for the working memory tasks.[26] The eight-arm radial maze (8-ARM) test was performed also in the same cohort at 9 and 13 months.[27] The number of correct choices in the initial eight chosen arms and the number of errors (defined as choosing arms already visited) were assessed. After all behavior examinations, TgTau$^{P301L(O)}$ and non-Tg littermates were examined histologically. Among TgTau$^{P301L(O)}$ mice, ~37% had pretangles; 42% had pretangles and GFTs; and 21% had pretangles, GFTs, and NFTs. Two cohorts of old TgTau^{P301L} mice and their non-Tg littermates were studied in Toronto (TgTau$^{P301L(T)}$). The first cohort (16 Tg and 10 non-Tg littermates) was 16 to 18 months of age, and the second cohort (13 Tg and six non-Tg littermates) was 16 months of age. Each cohort of mice was administered a battery of behavioral tests in the following sequence: an open-field test, a reference memory, and a cued (visible platform) version of the MWM test, followed by a conditioned taste aversion (CTA) test.[28,29] After all behavioral tests, the ratio of insoluble to soluble human tau in the brains of TgTau$^{P301L(T)}$ and non-Tg littermates was examined by Western blotting.

Statistical Analysis

For statistical analysis, two-way repeated measure analysis of variance with post hoc tests or the unpaired Student's *t*-test was performed (SPSS version 12 and GraphPad Prism version 4) as indicated in the text or as described in detail in the Supplementary Material (see *http://ajp.amjpathol.org*).

Results

NFTs, GFTs, and Phenotypic Variation in TgTau^{P301L} Mice

TgTau^{P301L} mice were derived from a series of microinjections also involving wt and TauR406W constructs. All constructs were based on a cDNA encoding the longest from of human tau (2N, 4R) inserted into the cos.Tet hamster PrP cosmid expression vector (Figure 1), with pathologies in some resultant TgTau^{R406W} lines being described previously.[23] From 3 months of age onwards, TgTau^{P301L} mice showed prominent dot-like tau immunoreactivity in the neurons of the pyramidal cell layers of the hippocampus (Figure 2a), amygdala, and cerebral cortex. Thereafter, tau immunoreactivity in TgTau^{P301L} mice spread and progressed with age. By 10 months of age, tau-positive pretangles were observed in numerous neurons. By 12 months of age, perineural or flame-shaped NFTs were observed in the cerebral cortex (Figure 2c), hippocampus, amygdala, basal forebrain nucleus, locus ceruleus, and substantia nigra. NFTs were labeled by Gallyas-Braak (Figure 2d), Bielschowsky (Figure 2e), and thioflavin-S (Figure 2f) staining procedures. The antibodies PHF1, AT8, Alz50, and Ubi-Q-labeled NFTs and numerous neuropil threads (Figure 2, g–j). Staining with MC1 (Figure 2k), CP27 (Figure 2l), and Tg3 (Figure 2m) also detected NFTs in the cerebral cortex. We have not yet found any abnormalities associated with expression of normal human tau in aged mice of a comparable Tg wt line denoted TgTau(wt)25355, implying a crucial pathogenic role for the P301L mutation (not shown). In the spinal cord of TgTau^{P301L} mice, a small number of glial tangles were observed, but NFT formation was not apparent (Figure 2n).

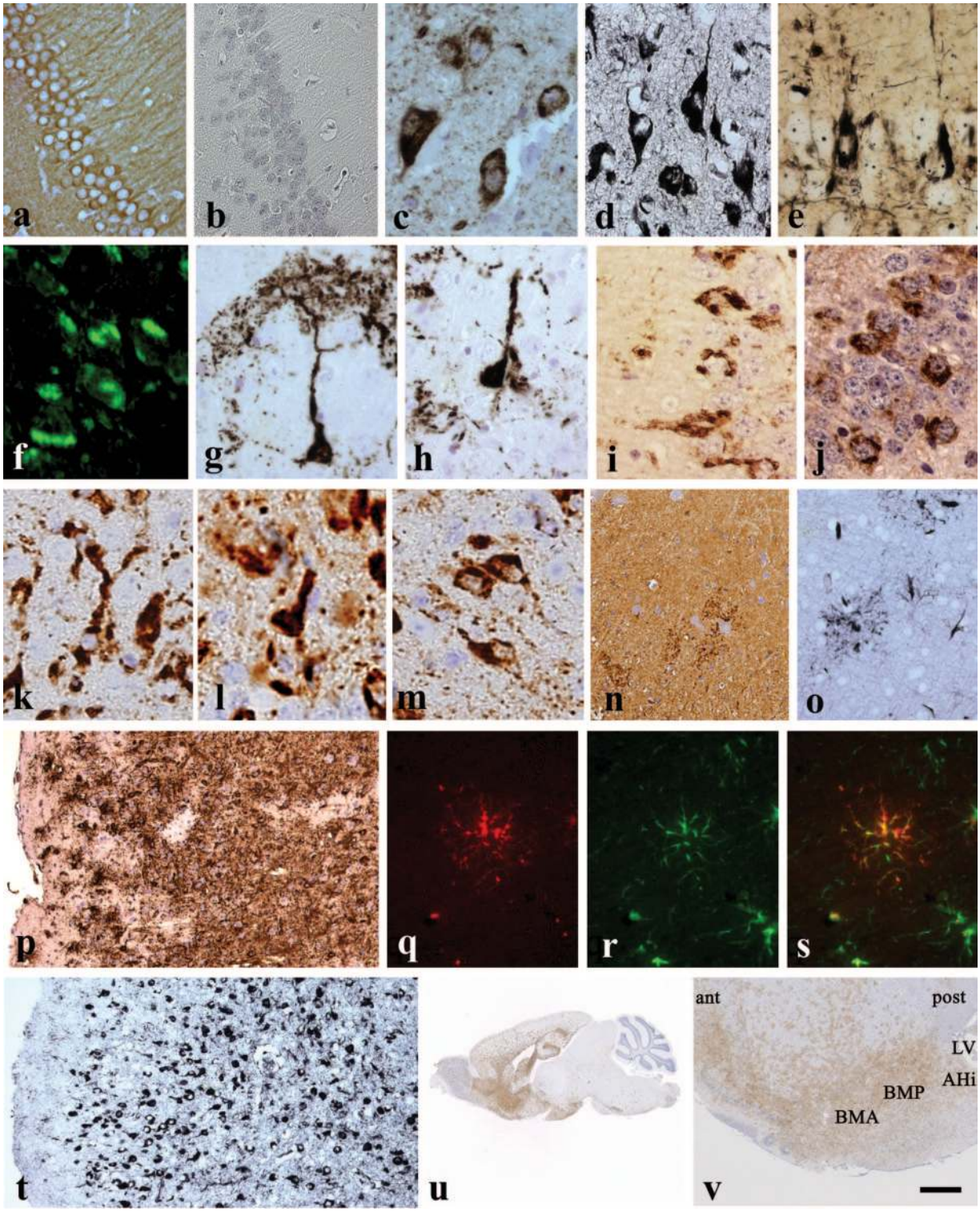

Figure 2. Tau pathologies in TgTau^{P301L} mouse brains. **a:** Dot-like immunoreactivity stained by Tau154 in hippocampal neurons of TgTau^{P301L} mice at 3 months of age. **b:** Neurons of age-matched non-Tg littermates did not show any signals. **c:** Prominent appearance of pretangles revealed by AT8 staining. **d:** Gallyas-Braak staining showed the NFTs, consisting of classic flame- or globose-type and perinuclear-type tangles. Many neuropil threads and coiled bodies were also observed. **e** and **f:** NFTs in the hippocampus stained by Bielschowsky (**e**) and thioflavin-S (**f**). **g–j:** PHF1- (**g**), AT8- (**h**), Alz50- (**i**), and Ubi-Q-labeled (**j**) NFTs, pretangles, and neuropil threads. **k–m:** Staining with MC1 (**k**), CP27 (**l**), and Tg3 (**m**) also detected NFTs in the cerebral cortex. **n:** A number of glial tangles are observed in the spinal cord, but neuronal tangles are not present. **o** and **p:** Extensive glial tangles consisted of astrocytic plaques detected by Gallyas-Braak (**o**) and antibody AT8 (**p**) staining in the frontotemporal cortex. **q–s:** Immunofluorescence study shows AT8 (**q**) and GFAP (**r**) are well co-localized (**s**). **t:** Gallyas-Braak staining showing prominent appearance of NFTs in the frontotemporal cortex. **u:** Lower power view of TgTau$^{P301L(T)}$ mouse showing extensive AT8 immunoreactivity in frontal areas in aged animals. This section is ~0.2 mm from the mid-line. **v:** Higher power view of a sagittal section ~2.5 mm from the mid-line to demonstrate the presence of NFTs and GFTs in the amygdaloid structures. BMA, basomedial amygdaloid nucleus; BMP, basomedial amygdaloid nucleus; AHi, amygdalohippocampal area; LV, large ventricle; ant, anterior; post, posterior. **a** and **b:** 3-month-old TgTau^{P301L} and wild-type mice; **c:** 12-month-old TgTau^{P301L}; **d–n** and **q–s:** 14-month-old TgTau^{P301L}; **o:** 8-month-old TgTau^{P301L}; **p:** 18-month-old TgTau^{P301L}; and **t–v:** 17-month-old TgTau^{P301L}. Scale bars = 93 μm (**a**, **b**); 187 μm (**c–m**, **o**, **q–s**); 374 μm (**n**); 47 μm (**p**, **t**); 2.5 mm (**u**); and 620 μm (**v**).

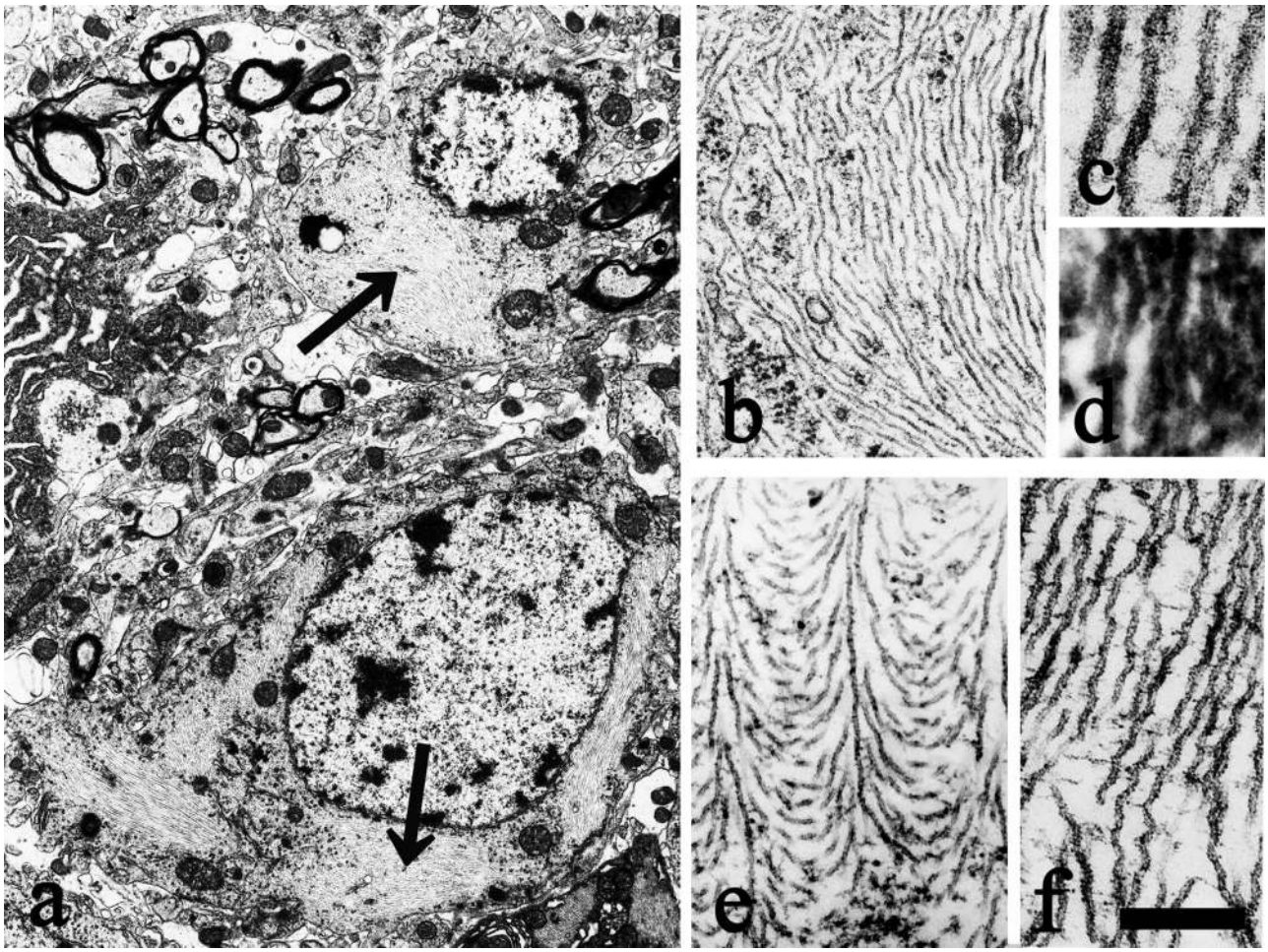

Figure 3. Electron microscopic study. **a:** Hippocampal neurons of 14-month-old TgTau^{P301L} mice with NFTs had wavy and straight tubules in the perikarya and proximal dendrites (**arrows**). **b:** Most of the tubules were composed of filaments 15 nm in width with a wavy appearance. These wavy tubules were almost longitudinally parallel and showed branching and crossover. **c:** Higher magnification of **b**. **d:** Antibody AT8 labeled these filaments viewed by immunoelectron microscopy. **e:** Peculiar crisscrossing straight filaments were observed. **f:** Astrocyte end-feet around the vessels were packed with wavy filaments. Scale bars = 2.4 mm (**a**); 0.5 μm (**b**); 0.1 μm (**c**); 0.2 μm (**d**); 0.3 μm (**e**); 0.1 μm (**f**).

Interestingly, florid glial tau pathology occurred independently of (and typically preceded) neuronal tau cytopathology. At 8 months of age, tufted astrocytes and plaque-like deposits were detected in the cerebral cortex (Figure 2o), hippocampus, striatum, brainstem, and spinal cord. The glial plaques were observed in the cerebral cortex of ~52% of the TgTau^{P301L} older than 12 months of age and closely resembled those seen in CBD or PSP. In some affected animals, fields of glial pathology merged to yield almost confluent immunostaining (Figure 2p). Immunofluorescence study revealed that most of the plaque-like deposits were stained with both AT8 and GFAP (Figure 2, q–s), suggesting that these tau deposits were mainly in astrocytes. The cytoplasm of some oligodendrocytes also showed immunoreactivity for AT8, although the appearance was different from that of the astrocytic plaques (not shown). In homozygous Tg mice, NFTs started to appear at 4 months of age and increased in severity with age, but the rate of appearance of NFTs and GFTs was ~50% in the homozygous TgTau^{P301L} mice even in the late phase of the disease course.

NFTs were extensively observed in the frontotemporal cortex and amygdala at 18 to 24 months of age (Figure 2t). Classic flame-type NFTs in the cortex and globose-type NFTs in the brainstem were also observed. Approximately 27% of TgTau^{P301L} mice older than 12 months of age showed NFTs. Although spinal cord and brainstem pathological features were prominent in previous reports of Tg Tau mice, the severity of cumulative neuropathology in the cortex of aged TgTau^{P301L} mice was remarkable. A low-power view of a 17-month-old heterozygote immunostained with AT8 antibody showed extensive immunostaining corresponding to the appearance of NFTs and GFTs in the hippocampus, frontal cortex, caudate, and accumbens nucleus (Figure 2, u and v).

In electron microscopy analyses, massive wavy tubules in the perikarya and proximal dendrites were seen in both the cortical and hippocampal neurons (Figure 3a, arrows). Most tubules were composed of filaments 12 to 22 nm wide and had a wavy appearance. Because the distance between the crossovers of the twist was variable, periodicity was not determined. These wavy tubules

were in longitudinally parallel arrays, although they showed branching and crossover (Figure 3, b and c). Immunoelectron microscopy showed that antibody AT8 labeled these filaments (Figure 3d). Aggregates of criss-crossing straight filaments (herringbone-like structure)[30] were observed (Figure 3e). Astrocytic end-feet around the vessels were packed with wavy filaments (Figure 3f).

Neurodegeneration in TgTau^{P301L} Brains

TgTau^{P301L} showed brain atrophy by 18 months (Figure 4a), whereas non-Tg littermates did not (Figure 4b). Atrophy was especially prominent in the temporal lobe [Figure 4, a (arrow) and c] and hippocampus (Figure 4a, arrowhead). Nissl staining in the hippocampus, amygdala, and the entorhinal cortex showed neurons with degenerated cytoplasm and condensed nuclei. The severity of degeneration paralleled the frequency of NFTs, neuropil threads, and GFTs. Synaptic density was reduced throughout the hippocampus (Figure 4d). In some TgTau^{P301L} mice, neuronal degeneration was so severe that neurons in the pyramidal cell layer in CA1 and CA2 almost disappeared (Figure 4, e and f). Severe reactive astrocytosis (Figure 4h) was also detected.

Tau Expression and Insoluble Tau Aggregates in TgTau^{P301L} Brains

The net expression level of tau in TgTau^{P301L} mice detected by tau-C was 1.7 times that of endogenous mouse tau at 4 months of age (Figure 5a). Western blotting using Tau154 showed the specific expression of a 68-kd band, the longest spliced form of human tau, in the Tris saline-soluble fractions, with the levels being similar in the cortical areas, hippocampus, basal ganglia, cerebellum, brainstem, and spinal cord. With aging, sarkosyl-insoluble forms of human tau became apparent and were phosphorylated in many regions of the central nervous system in Tg mice but were especially increased in the cortical areas, hippocampus, and basal ganglia (Figure 5b). However, more marked phenotypic variation was seen in the accumulation of sarkosyl-insoluble tau compared with soluble tau. The amount of insoluble tau was correlated with the histopathological severity detected by AT8 (Figure 5c). Pair-wise analysis of two TgTau^{P301L} mice with either low or high histopathology showed prominent enhancement of NFT-specific conformational changes (Tg3, Alz50, MC1) and phosphorylation (AT8, PHF1) in the accumulated insoluble tau (Figure 5d).

Working Memory Disturbance Assessed in MWM and 8-ARM Tests

Extensive behavioral testing showed no gross motor deficits in TgTau$^{P301L(O)}$ or TgTau$^{P301L(T)}$ mice. Spatial reference memory, as measured by the MWM test, was normal in TgTau$^{P301L(O)}$ mice at 9 or 12 months of age [TgTau$^{P301L(O)}$ and non-Tg littermates, $P = 0.3$; Figure 6a]. Similarly, spatial reference memory and performance in the cued (visible platform) version of the MWM test was normal in TgTau$^{P301L(T)}$ mice at 17 months of age ($P = 0.001$; see also Supplementary Data at http://ajp.amjpathol.org). However, working memory (measured at 12 months of age in the MWM test and at 13 months of age in the 8-ARM test) was significantly disturbed in the TgTau$^{P301L(O)}$ group compared with non-Tg littermates. In the MWM task, TgTau$^{P301L(O)}$ mice displayed a longer path length and a longer latency to find the platform than non-Tg littermates (path length, $P < 0.05$; latency, $P < 0.05$; Figure 6b). In the 8-ARM test, TgTau$^{P301L(O)}$ mice made significantly fewer correct choices ($P < 0.001$; Figure 6c) and a greater number of errors ($P < 0.001$; Figure 6d); as assessed by a two-way repeated measure analysis of variance. Post hoc analyses showed that performance on this task declined over blocks five or six in TgTau$^{P301L(O)}$ mice. These disturbances were more prominent in TgTau$^{P301L(O)}$ mice with GFTs or NFTs compared with TgTau$^{P301L(O)}$ mice with only pretangles in the brain ($P < 0.05$; Figure 6e).

Memory Disturbance Assessed in CTA Tests

In the CTA paradigm, the ingestion of a novel taste (saccharine) is paired with transient sickness (produced by injection of LiCl). Memory for this association is evident when the animal avoids that taste on subsequent presentations. TgTau$^{P301L(T)}$ mice, ages 16 to 18 months, and non-Tg littermates were tested for CTA. In the memory test conducted 2 days after the pairing, saccharine consumption in non-Tg mice was significantly below chance levels ($P < 0.001$; Figure 7a), indicating robust memory for the association, whereas saccharine consumption by TgTau$^{P301L(T)}$ mice was not different from chance levels ($P > 0.05$), indicating impaired memory. In control mice that were treated similarly except that the novel taste (saccharine) was not paired with transient sickness (mice were injected with buffered saline rather than LiCl), both TgTau$^{P301L(T)}$ and non-Tg littermates showed comparable saccharine intake (Figure 7b; $P = 0.08$), indicating that the TgTau$^{P301L(T)}$ mice do not have an unconditioned performance for saccharine. Therefore, pairing the novel taste with LiCl produces robust CTA memory in non-Tg animals but not in Tg mice. One intriguing finding is that TgTau$^{P301L(T)}$ mice showed considerable heterogeneity in their memory for CTA. Tg mice with ratios (1 or higher) of insoluble to soluble human tau protein exhibited the most severe impairments (Figure 7, c and d; see also Supplementary Data at *http://ajp.amjpathol.org*).

Discussion

TgTau^{P301L} mice show numerous NFTs and GFTs in the brain. In some of the severely affected mice, neuronal degeneration was also observed. The results of immunostaining and immunoblot analysis suggest that the mice have age-related accumulation of tau protein with special properties, such as hyperphosphorylation, ubiquitinylation, conformational alteration, and sarkosyl insolubility,

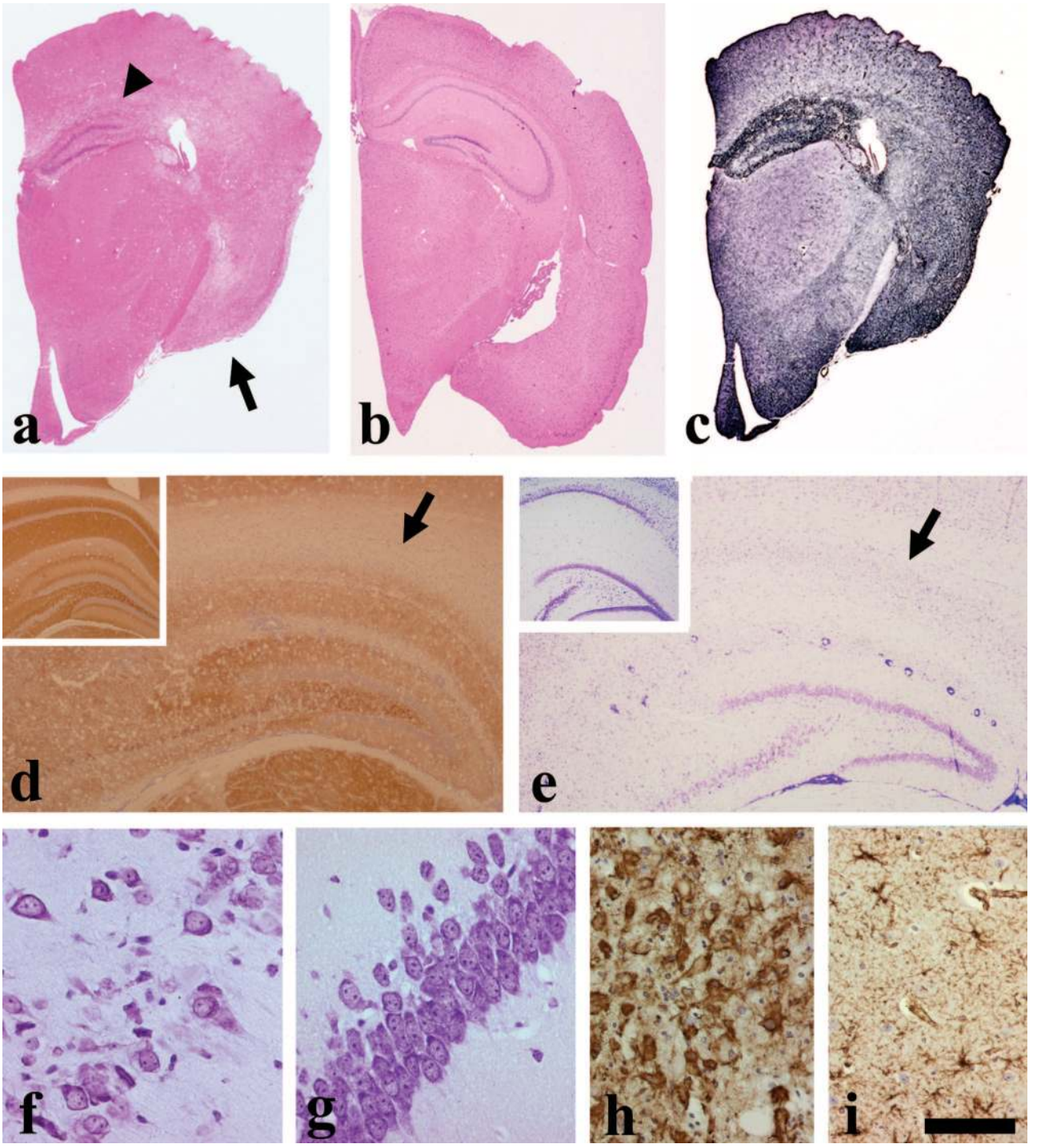

Figure 4. Severe stage of tau pathology in TgTau^{P301L} mice. **a** and **b:** Prominent atrophy of temporal lobe (**a**, **arrow**) and hippocampus (**a**, **arrowhead**) in 18-month-old TgTau^{P301L} mice compared with that in age-matched non-Tg littermates (**b**) by H&E staining. Gallyas-Braak staining showed prominent tau pathology in 18-month-old TgTau^{P301L} mice. **c:** Note the extensive appearance of NFTs and GFTs that were labeled with prominent blue staining in TgTau^{P301L} mice. **d:** Remarkable decrease of synaptic density (synaptophysin staining) in TgTau^{P301L} mice (**arrow**) compared with non-Tg littermates (top left). **e:** The disappearance of the pyramidal cell layer in CA1 and CA2 and severe degeneration of neurons in CA3 (**arrow**) revealed by Nissl staining compared with non-Tg littermates (top left). **f:** Higher magnification of severe neuronal degeneration and loss in CA1 of other TgTau^{P301L} at 18 months of age (Nissl stain). **g:** Note that the CA1 neurons of non-Tg littermates were preserved. **h** and **i:** Prominent GFAP-positive reactive astrocytes in the hippocampus of TgTau^{P301L} mice (**h**) yet mild astrocytosis in the same location in non-Tg littermates (**i**). Scale bars = 800 μm (**a–c**); 500 μm (**d**, **e**); 50 μm (**h**, **g**); 100 μm (**h**, **i**).

as is present in FTDP-17.[3,11] FTDP-17 patients with the tau P301L mutation show both paired helical filaments, with a diameter of 15 nm and a periodicity of 130 nm, and small proportion of straight filaments of ~12 nm in diameter.[3,10,31] Our TgTau^{P301L} mice showed wavy filaments and sometimes had aggregates of criss-crossing straight filaments in the perikarya, proximal dendrites of neurons, and astrocytes, and these filaments resembled filaments

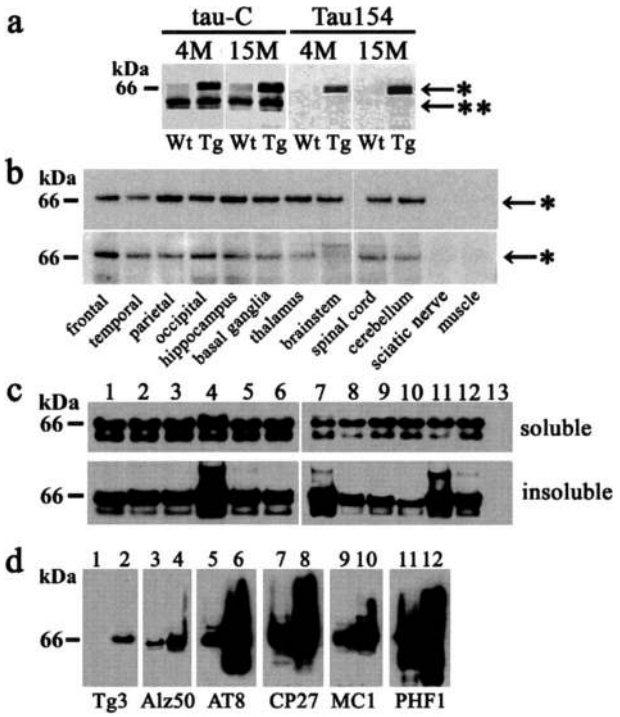

Figure 5. Transgene-encoded tau proteins. **a:** Tris saline-soluble fractions of TgTau^{P301L} (Tg) and non-Tg littermates (Wt). Expression levels of mutant tau detected with antibody tau-C (*) were 1.7 times higher at 4 months of age and 4.8 times higher at 15 months of age in TgTau^{P301L} mice compared with those of endogenous mouse tau (**) (tau-C). Endogenous mouse tau was not detected with the human-specific 154 antibody (Tau154). **b:** Sarkosyl-insoluble fraction of 15-month-old TgTau^{P301L} mice. Sarkosyl-insoluble tau was accumulated in all regions of the central nervous system, especially in the cortical areas, hippocampus, and basal ganglia (top: *, antibody Tau154; bottom: *, antibody PS199). **c:** Phenotypic variation detected with CP27 antibody in the accumulation of sarkosyl soluble tau (top) compared with insoluble tau (bottom) in TauTg^{P301L} mice at 19 months of age (Tg mice: **lanes 1** to **12** and a non-Tg control, **lane 13**). Note the variation among age-matched animals, with high levels of accumulation prominent in animals represented by **lanes 4**, **7**, and **11**. **d:** Pair-wise analysis of two Tg^{P301L} mice with either low or high histopathology (odd- and even-numbered lanes, respectively, as assessed with AT8 antibody) showed prominent enhancement of NFT-specific conformational changes (Tg3, Alz50, MC1) and phosphorylation (AT8, PHF1) in the accumulated insoluble tau.

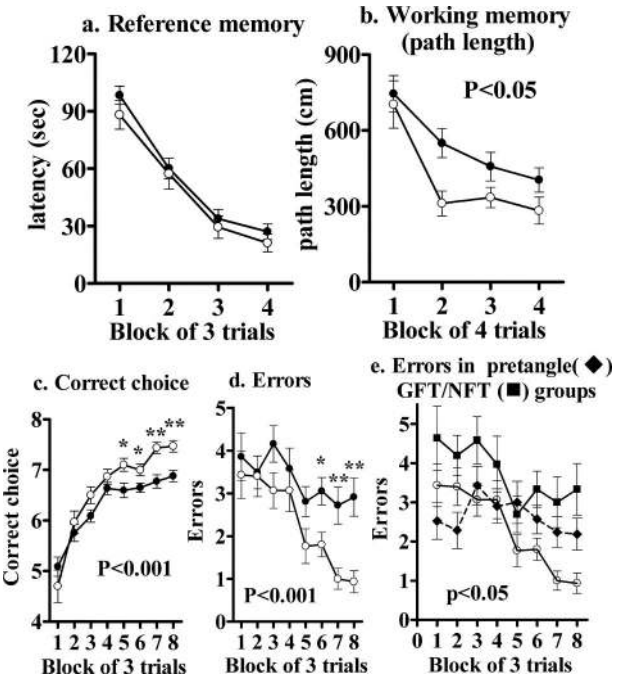

Figure 6. MWM and 8-ARM tests. In the MWM test performed at age 12 months, each TgP301L(O) mouse received three trials daily for 3 consecutive days for the reference memory task. For the working memory task, four different platform locations and starting positions were used. A block consisted of four trials, and each mouse was subjected to one block daily for 5 consecutive days. **a:** There was no significant difference between TgTau$^{P301L(O)}$ and non-Tg littermates in the reference memory task (P = 0.3). **b:** In the working memory task, spatial learning ability was significantly disturbed in the TgTau$^{P301L(O)}$ group compared with the non-Tg littermates ($P < 0.05$). TgTau$^{P301L(O)}$; ●, n = 12; non-Tg littermates: ○, n = 19. **c:** In the 8-ARM test at 13 months of age, a block consisted of three trials and each mouse was subjected to one trial daily for 8 consecutive days. Both groups gradually increased the correct choices (**c**) and decreased the errors (**d**). However, significant differences were recognized in the number of correct choices ($P < 0.001$) and the number of errors ($P < 0.001$) between TgTau$^{P301L(O)}$ and non-Tg littermates by two-way repeated analysis of variance. A post hoc test showed that spatial memory declined from five (**c**) or six blocks (**d**) in TgTau$^{P301L(O)}$ mice. **e:** These disturbances were more prominent in TgTau$^{P301L(O)}$ mice with GFTs or NFTs compared with TgTau$^{P301L(O)}$ mice with only pretangles in the brain ($P < 0.05$). TgTau$^{P301L(O)}$; ●, n = 10; non-Tg littermates: ○, n = 19; TgTau$^{P301L(O)}$ mice with pretangles plus GFTs or pretangles plus GFTs and NFTs: ■, n = 12; TgTau$^{P301L(O)}$ mice with only tau-positive pretangles; ◆, n = 7. *$P < 0.05$, **$P < 0.01$.

observed in FTDP-17.[32–34] Thus, TgTau^{P301L} mice exhibit pathological and biochemical features that are well correlated with those of FDTP-17. These tau pathologies were especially prominent in the cerebral cortices, hippocampus, and amygdala. The accumulation of aggregated tau protein was finally accompanied by neuronal loss in the brains of severely affected TgTau^{P301L} mice. All these findings implicate that the TgTau^{P301L} mice are a useful animal model with recapitulation of the tau pathologies seen in FTDP-17.

Histological studies have revealed significant overlap among FTDP-17, Pick's disease, CBD, PSP, and AD patients.[35,36] A pathological diagnosis of CBD or PSP is often given to FTDP-17 patients. Such diagnoses occur because, for instance, the appearance of GFTs is one of the characteristics of CBD and PSP, as well as of FTDP-17.[3,37] Flame-type NFTs in the cortex and globose-type NFTs in the brainstem are also hallmarks of CBD and PSP. These findings suggest that TgTau^{P301L} mice also show pathological variations commonly recognized in PSP and CBD.

Given that the hamster PrP promoter is associated with pan-neuronal expression in the central nervous system, the appearance of florid astrocytic pathology in TgTau^{P301L} mice was unexpected. Nonetheless, astrocytic expression has been documented previously for hamster PrP mRNA,[38] and the potent accumulation of GFTs may represent an inability of this lineage to deal with abnormal forms of tau. Although several reports have detected glial pathologies of transgenic tau mice,[39–41] glial pathology in our TgTau^{P301L} mice is remarkable. Another unexpected feature of TgTau^{P301L} mice was variance in phenotypic manifestation, standing in marked contrast to our experience with the amyloid precursor protein Tg mice that were constructed via similar methodologies.[26] One manifestation of variance was the uncoupled appearance of neuronal and glial pathologies. Although all TgTau^{P301L} mice exhibited numerous tau-positive pretangles, GFTs appeared in ~20% of young (8

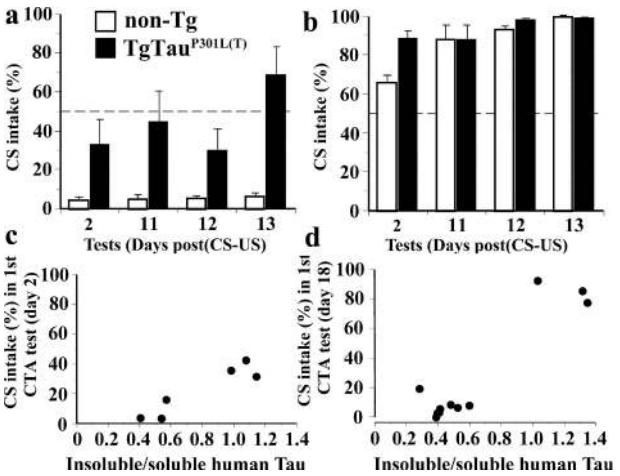

Figure 7. CTA tests. **a:** TgTau$^{P301L(T)}$ mice showed impaired learning of taste aversion as compared with non-Tg littermates ($P < 0.01$). Pairing of a novel taste (conditioned stimulus, CS) with an experimentally induced unconditioned stimulus (US, mildly noxious intraperitoneal injection of LiCl solution) resulted in a significant avoidance of CS (evaluated against 50% chance level; $P < 0.001$ for all test days) by non-Tg mice. In contrast, the TgTau$^{P301L(T)}$ mice consumed CS at the 50% chance level. **b:** The expression of the mutated human P301L gene did not affect the preference for a sweet solution in the Tg mice. Both Tg and non-Tg unconditioned mice showed a steady preference for CS during all tests. Although non-Tg mice showed an initial neophobic response to a novel taste of CS during the first test, they showed strong saccharine intake in later tests comparable with that in TgTau$^{P301L(T)}$ mice. **c:** The TgTau$^{P301L(T)}$ mice in the first tested cohort showed a positive association between the CS intake and brain pathology. **d:** Similarly, the association between the CS intake and brain pathology was also positive in the second cohort of mice. In both experiments, mice with higher ratios of insoluble to soluble tau fractions (~1 or higher) failed to learn the CS-US association, whereas mice with lower levels of insoluble tau fraction demonstrated stronger initial learning of the CS-US association. Pearson product-moment correlation coefficients $r = 0.93$, $P < 0.01$, and $r = 0.92$, $P < 0.001$, were found for **c** and **d**, respectively.

months old) and 50% of aged (18 to 22 months old) heterozygous TgTau$^{P301L(O)}$ mice. NFTs were observed in 18 to 27% of the aged mice. A second manifestation was apparent from different ages of onset to florid pathology in mice from the colonies denoted TgTau$^{P301L(O)}$ and TgTau$^{P301L(T)}$ mice. Lastly, there was within-cohort variance in pathology measured at an intermediate stage of the disease. The asynchronous development of pathology was also accompanied by variable performance in the 8-ARM and CTA tests (Figures 6 and 7). However, a gender effect on phenotypic variation was not apparent in our TgTau^{P301L} mice. The origin of the variance present within both male and female mice is unclear, but variable transgene expression levels are unlikely to be a causative factor because 1) the two Tg colonies yielded similar levels of overexpression (170%); 2) levels of soluble tau were similar among littermates (Figure 5); 3) there have been no indications of fluctuating transgene copy number during 4 years of experience with the TgTau$^{P301L(T)}$ line (not shown); and 4) the cos.Tet prion vector has found wide usage precisely because it engenders position-independent transgene expression (ie, it is not susceptible to integration site variegation effects). On the other hand, we note that a phenomenon of variable penetrance was also apparent for TauR406W mice,[23] suggesting this outcome could represent an intrinsic facet of the biology of pathogenic forms of tau. It is well known that there is large variation in the clinical and neuropathological features of the disease even within families with the same P301L mutation.[7,10,12,42] The variance both in human families with FTDP-17 and in our mice may be attributable to genetic modifiers, or to environmental parameters, or to some variety of stress condition. Actually, several studies have suggested that tau phosphorylation is influenced in animals subjected to stress.[43,44] With regards to the genetics of FTDP-17, mutant APP, ApoE, or Pin-1 have been suggested to modify the development of tau pathology.[10,42] Identification of genetic or environmental factors using the current mouse model will therefore be of great interest.

To the best of our knowledge, the TgTau^{P301L} mouse is an excellent tauopathy model with rampant pathologies in both astrocytes and neurons, yet showing decline in memory tasks before any confounding motor impairments. TgTau^{P301L} mice exhibit disturbances of hippocampal-dependent spatial working memory, as well as hippocampal-independent associative learning. CTA is dependent on the amygdala as well as the gustatory pathway, which involves the agranular insular cortex.[28,29] Interestingly, these disturbances were closely correlated with the presence of GFTs and NFTs in the 8-ARM test and the severity of insoluble tau accumulation in the CTA test (Figures 6 and 7). In the first reported Tg mice expressing the shortest 4R tau (4R0N) with the P301L mutation, Gallyas-Braak-positive NFTs with filamentous aggregates appeared in the spinal cord, and amyotrophic motor disturbance was observed.[12] However, progressive motor weakness prevented the mice from being tested for memory function. Another P301L Tg line exhibited NFTs and neuronal loss in the anterior spinal cord,[13] but impaired performance in CTA occurred in the absence of tangle pathologies.[28] Typical Alzheimer-paired helical filaments and half-twisted ribbons in FTDP-17 with reduction of motor neurons have already been shown in the brains of transgenic mice expressing alternatively spliced forms of wt human tau in the absence of endogenous mouse tau isoforms[45] and in the spinal cords of human P301S tau transgenic mice,[46] respectively, but cognitive performance was not assessed in either case. Age-dependent appearance of pretangles, mature tangles, and neuronal loss with brain atrophy and cognitive deficits was reproduced in recent tau P301L transgenic mice with 7× or 13× overexpression.[15] In this model, the suppression of transgenic tau partially alleviated memory disturbance and attenuated neurodegeneration, suggesting that NFTs are not sufficient to cause cognitive decline or neuronal death. In the present study, TgTau^{P301L} mice with 1.7× overexpression also showed age-dependent cortical tau pathology. Hippocampal-dependent and -independent cognitive deficits were revealed before the appearance of any motor disturbances. Furthermore, prominent neuronal and glial tau pathology and phenotypic variation, which are often observed in FTDP-17, were also seen in our TgTau^{P301L} mice. Although a number of transgenic mice expressing human tau have been reported to show glial pathology,[39–41] the TgTau^{P301L} line described here is unique with regards to the development of florid glial plaques. Because memory disturbances were correlated with the

levels of GFTs or NFTs rather than with those of only pretangles, glial tau pathology may contribute to hippocampal-dependent and -independent cognitive deficit in TgTau^{P301L} mice. Our TgTau^{P301L} mice did not show prominent tau accumulation in spinal motor neurons (Figure 2n), and this is presumably why the mice do not show gross motor impairment.

In conclusion, TgTau^{P301L} mice recapitulate pathological, biochemical, and behavioral changes observed in FTDP-17 with the P301L mutation, with some pathological features also resembling those of CBD and PSP. Because TgTau^{P301L} mice develop an initial tau accumulation in neurons and glial cells, followed by tangle formation and accompanied by memory disturbances, they will be useful for investigating all of the aspects of this pathological cascade. They may also be of considerable use for evaluating possible new curable therapeutic agents for FTDP-17 and other tauopathies including AD, PSP, and CBD.

Acknowledgments

We thank Y. Nogami and H. Narihiro for technical assistance; Dr. H. Kawabe for behavioral examinations; Dr. Dennis W. Dickson for the antibody Ubi-Q; Dr. Peter Davies for the antibodies CP27, Tg3, and MC1; and Dr. Sheena Josselyn for helpful discussions.

References

1. Foster NL, Wilhelmsen K, Sima AA, Jones MZ, D'Amato CJ, Gilman S: Frontotemporal dementia and parkinsonism linked to chromosome 17: a consensus conference. Conference Participants. Ann Neurol 1997, 41:706–715
2. Spillantini MG, Murrell JR, Goedert M, Farlow MR, Klug A, Ghetti B: Mutation in the tau gene in familial multiple system tauopathy with presenile dementia. Proc Natl Acad Sci USA 1998, 95:7737–7741
3. Mirra SS, Murrell JR, Gearing M, Spillantini MG, Goedert M, Crowther RA, Levey AI, Jones R, Green J, Shoffner JM, Wainer BH, Schmidt ML, Trojanowski JQ, Ghetti B: Tau pathology in a family with dementia and a P301L mutation in tau. J Neuropathol Exp Neurol 1999, 58:335–345
4. Lippa CF, Zhukareva V, Kawarai T, Uryu K, Shafiq M, Nee LE, Grafman J, Liang Y, St. George-Hyslop PH, Trojanowski JQ, Lee VM: Frontotemporal dementia with novel tau pathology and a Glu342Val tau mutation. Ann Neurol 2000, 48:850–858
5. Pickering-Brown SM, Richardson AM, Snowden JS, McDonagh AM, Burns A, Braude W, Baker M, Liu WK, Yen SH, Hardy J, Hutton M, Davies Y, Allsop D, Craufurd D, Neary D, Mann DM: Inherited frontotemporal dementia in nine British families associated with intronic mutations in the tau gene. Brain 2002, 125:732–751
6. Neumann M, Schulz-Schaeffer W, Crowther RA, Smith MJ, Spillantini MG, Goedert M, Kretzschmar HA: Pick's disease associated with the novel Tau gene mutation K369I. Ann Neurol 2001, 50:503–513
7. Bugiani O, Murrell JR, Giaccone G, Hasegawa M, Ghigo G, Tabaton M, Morbin M, Primavera A, Carella F, Solaro C, Grisoli M, Savoiardo M, Spillantini MG, Tagliavini F, Goedert M, Ghetti B: Frontotemporal dementia and corticobasal degeneration in a family with a P301S mutation in tau. J Neuropathol Exp Neurol 1999, 58:667–677
8. Morris HR, Osaki Y, Holton J, Lees AJ, Wood NW, Revesz T, Quinn N: Tau exon 10 +16 mutation FTDP-17 presenting clinically as sporadic young onset PSP. Neurology 2003, 61:102–104
9. Rizzu P, Joosse M, Ravid R, Hoogeveen A, Kamphorst W, van Swieten JC, Willemsen R, Heutink P: Mutation-dependent aggregation of tau protein and its selective depletion from the soluble fraction in brain of P301L FTDP-17 patients. Hum Mol Genet 2000, 9:3075–3082
10. Bird TD, Nochlin D, Poorkaj P, Cherrier M, Kaye J, Payami H, Peskind E, Lampe TH, Nemens E, Boyer PJ, Schellenberg GD: A clinical pathological comparison of three families with frontotemporal dementia and identical mutations in the tau gene (P301L). Brain 1999, 122:741–756
11. Nasreddine ZS, Loginov M, Clark LN, Lamarche J, Miller BL, Lamontagne A, Zhukareva V, Lee VM, Wilhelmsen KC, Geschwind DH: From genotype to phenotype: a clinical pathological, and biochemical investigation of frontotemporal dementia and parkinsonism (FTDP-17) caused by the P301L tau mutation. Ann Neurol 1999, 45:704–715
12. Lewis J, McGowan E, Rockwood J, Melrose H, Nacharaju P, Van Slegtenhorst M, Gwinn-Hardy K, Paul Murphy M, Baker M, Yu X, Duff K, Hardy J, Corral A, Lin WL, Yen SH, Dickson DW, Davies P, Hutton M: Neurofibrillary tangles, amyotrophy and progressive motor disturbance in mice expressing mutant (P301L) tau protein. Nat Genet 2000, 25:402–405
13. Götz J, Chen F, Barmettler R, Nitsch RM: Tau filament formation in transgenic mice expressing P301L tau. J Biol Chem 2001, 276:529–534
14. Tanemura K, Murayama M, Akagi T, Hashikawa T, Tominaga T, Ichikawa M, Yamaguchi H, Takashima A: Neurodegeneration with tau accumulation in a transgenic mouse expressing V337M human tau. J Neurosci 2002, 22:133–141
15. Santacruz K, Lewis J, Spires T, Paulson J, Kotilinek L, Ingelsson M, Guimaraes A, DeTure M, Ramsden M, McGowan E, Forster C, Yue M, Orne J, Janus C, Mariash A, Kuskowski M, Hyman B, Hutton M, Ashe KH: Tau suppression in a neurodegenerative mouse model improves memory function. Science 2005, 309:476–481
16. Hutton M, Lendon CL, Rizzu P, Baker M, Froelich S, Houlden H, Pickering-Brown S, Chakraverty S, Isaacs A, Grover A, Hackett J, Adamson J, Lincoln S, Dickson D, Davies P, Petersen RC, Stevens M, de Graaff E, Wauters E, van Baren J, Hillebrand M, Joosse M, Kwon JM, Nowotny P, Che LK, Norton J, Morris JC, Reed LA, Trojanowski J, Basun H, Lannfelt L, Neystat M, Fahn S, Dark F, Tannenberg T, Dodd PR, Hayward N, Kwok JB, Schofield PR, Andreadis A, Snowden J, Craufurd D, Neary D, Owen F, Oostra BA, Hardy J, Goate A, van Swieten J, Mann D, Lynch T, Heutink P: Association of missense and 5′-splice-site mutations in tau with the inherited dementia FTDP-17. Nature 1998, 393:702–705
17. Clark LN, Poorkaj P, Wszolek Z, Geschwind DH, Nasreddine ZS, Miller B, Li D, Payami H, Awert F, Markopoulou K, Andreadis A, D'Souza I, Lee VM, Reed L, Trojanowski JQ, Zhukareva V, Bird T, Schellenberg G, Wilhelmsen KC: Pathogenic implications of mutations in the tau gene in pallido-ponto-nigral degeneration and related neurodegenerative disorders linked to chromosome 17. Proc Natl Acad Sci USA 1998, 95:13103–13107
18. Poorkaj P, Grossman M, Steinbart E, Payami H, Sadovnick A, Nochlin D, Tabira T, Trojanowski JQ, Borson S, Galasko D, Reich S, Quinn B, Schellenberg G, Bird TD: Frequency of tau gene mutations in familial and sporadic cases of non-Alzheimer dementia. Arch Neurol 2001, 58:383–387
19. Kozak M: An analysis of vertebrate mRNA sequences: intimations of translational control. J Cell Biol 1991, 115:887–903
20. Scott MR, Köhler R, Foster D, Prusiner SB: Chimeric prion protein expression in cultured cells and transgenic mice. Protein Sci 1992, 1:986–997
21. Citron M, Westaway D, Xia W, Carlson G, Diehl T, Levesque G, Johnson-Wood K, Lee M, Seubert P, Davis A, Kholodenko D, Motter R, Sherrington R, Perry B, Yao H, Strome R, Lieberburg I, Rommens J, Kim S, Schenk D, Fraser P, St. George Hyslop P, Selkoe DJ: Mutant presenilins of Alzheimer's disease increase production of 42-residue amyloid beta-protein in both transfected cells and transgenic mice. Nat Med 1997, 3:67–72
22. Basler K, Oesch B, Scott M, Westaway D, Wälchli M, Groth DF, McKinley MP, Prusiner SB, Weissmann C: Scrapie and cellular PrP isoforms are encoded by the same chromosomal gene. Cell 1986, 46:417–428
23. Ikeda M, Shoji M, Kawarai T, Kawarabayashi T, Matsubara E, Murakami T, Sasaki A, Tomidokoro Y, Ikarashi Y, Kuribara H, Ishiguro K, Hasegawa M, Yen SH, Chishti MA, Harigaya Y, Abe K, Okamoto K, St. George-Hyslop P, Westaway D: Accumulation of filamentous tau in the cerebral cortex of human tau R406W transgenic mice. Am J Pathol 2005, 166:521–531
24. Weaver CL, Espinoza M, Kress Y, Davies P: Conformational change

as one of the earliest alterations of tau in Alzheimer's disease. Neurobiol Aging 2000, 21:719–727
25. Murakami T, Shoji M, Imai Y, Inoue H, Kawarabayashi T, Matsubara E, Harigaya Y, Sasaki A, Takahashi R, Abe K: Pael-R is accumulated in Lewy bodies of Parkinson's disease. Ann Neurol 2004, 55:439–442
26. Janus C, Pearson J, McLaurin J, Mathews PM, Jiang Y, Schmidt SD, Chishti MA, Horne P, Heslin D, French J, Mount HT, Nixon RA, Mercken M, Bergeron C, Fraser PE, St. George-Hyslop P, Westaway D: A beta peptide immunization reduces behavioural impairment and plaques in a model of Alzheimer's disease. Nature 2000, 408:979–982
27. Egashira N, Tanoue A, Higashihara F, Mishima K, Fukue Y, Takano Y, Tsujimoto G, Iwasaki K, Fujiwara M: V1a receptor knockout mice exhibit impairment of spatial memory in an eight-arm radial maze. Neurosci Lett 2004, 356:195–198
28. Pennanen L, Welzl H, D'Adamo P, Nitsch RM, Götz J: Accelerated extinction of conditioned taste aversion in P301L tau transgenic mice. Neurobiol Dis 2004, 15:500–509
29. Janus C, Welzl H, Hanna A, Lovasic L, Lane N, St. George-Hyslop P, Westaway D: Impaired conditioned taste aversion learning in APP transgenic mice. Neurobiol Aging 2004, 25:1213–1219
30. Lewis J, Dickson DW, Lin WL, Chisholm L, Corral A, Jones G, Yen SH, Sahara N, Skipper L, Yager D, Eckman C, Hardy J, Hutton M, McGowan E: Enhanced neurofibrillary degeneration in transgenic mice expressing mutant tau and APP. Science 2001, 293:1487–1491
31. Reed LA, Wszolek ZK, Hutton M: Phenotypic correlations in FTDP-17. Neurobiol Aging 2001, 22:89–107
32. Spillantini MG, Crowther RA, Kamphorst W, Heutink P, van Swieten JC: Tau pathology in two Dutch families with mutations in the microtubule-binding region of tau. Am J Pathol 1998, 153:1359–1363
33. van Swieten JC, Stevens M, Rosso SM, Rizzu P, Joosse M, de Koning I, Kamphorst W, Ravid R, Spillantini MG, Niermeijer, Heutink P: Phenotypic variation in hereditary frontotemporal dementia with tau mutations. Ann Neurol 1999, 46:617–626
34. Miyasaka T, Morishima-Kawashima M, Ravid R, Kamphorst W, Nagashima K, Ihara Y: Selective deposition of mutant tau in the FTDP-17 brain affected by the P301L mutation. J Neuropathol Exp Neurol 2001, 60:872–884
35. Feany MB, Dickson DW: Neurodegenerative disorders with extensive tau pathology: a comparative study and review. Ann Neurol 1996, 40:139–148
36. Feany MB, Mattiace LA, Dickson DW: Neuropathologic overlap of progressive supranuclear palsy, Pick's disease and corticobasal degeneration. J Neuropathol Exp Neurol 1996, 55:53–67
37. Komori T, Arai N, Oda M, Nakayama H, Mori H, Yagishita S, Takahashi T, Amano N, Murayama S, Murakami S, Shibata N, Kobayashi M, Sasaki S, Iwata M: Astrocytic plaques and tufts of abnormal fibers do not coexist in corticobasal degeneration and progressive supranuclear palsy. Acta Neuropathol (Berl) 1998, 96:401–408
38. Moser M, Colello RJ, Pott U, Oesch B: Developmental expression of the prion protein gene in glial cells. Neuron 1995, 14:509–517
39. Lin WL, Lewis J, Yen SH, Hutton M, Dickson DW: Filamentous tau in oligodendrocytes and astrocytes of transgenic mice expressing the human tau isoform with the P301L mutation. Am J Pathol 2003, 162:213–238
40. Higuchi M, Ishihara T, Zhang B, Hong M, Andreadis A, Trojanowski J, Lee VM: Transgenic mouse model of tauopathies with glial pathology and nervous system degeneration. Neuron 2002, 35:433–446
41. Götz J, Tolnay M, Barmettler R, Chen F, Probst A, Nitsch RM: Oligodendroglial tau filament formation in transgenic mice expressing G272V tau. Eur J Neurosci 2001, 13:2131–2140
42. Lee VM, Goedert M, Trojanowski JQ: Neurodegenerative tauopathies. Annu Rev Neurosci 2001, 24:1121–1159
43. Goedert M, Hasegawa M, Jakes R, Lawler S, Cuenda A, Cohen P: Phosphorylation of microtubule-associated protein tau by stress-activated protein kinases. FEBS Lett 1997, 409:57–62
44. Okawa Y, Ishiguro K, Fujita SC: Stress-induced hyperphosphorylation of tau in the mouse brain. FEBS Lett 2003, 535:183–189
45. Andorfer C, Kress Y, Espinoza M, de Silva R, Tucker KL, Barde YA, Duff K, Davies P: Hyperphosphorylation and aggregation of tau in mice expressing normal human tau isoforms. J Neurochem 2003, 86:582–590
46. Allen B, Ingram E, Takao M, Smith MJ, Jakes R, Virdee K, Yoshida H, Holzer M, Craxton M, Emson PC, Atzori C, Migheli A, Crowther RA, Ghetti B, Spillantini MG, Goedert M: Abundant tau filaments and nonapoptotic neurodegeneration in transgenic mice expressing human P301S tau protein. J Neurosci 2002, 22:9340–9351